



HAL
open science

Competition Between Steric Hindrance and Hydrogen Bonding in the Formation of Supramolecular Bottle Brush Polymers

Sylvain Catrouillet, Cécile Fonteneau, Laurent Bouteiller, Nicolas Delorme, Erwan Nicol, Taco Nicolai, Sandrine Pensec, Olivier Colombani

► **To cite this version:**

Sylvain Catrouillet, Cécile Fonteneau, Laurent Bouteiller, Nicolas Delorme, Erwan Nicol, et al.. Competition Between Steric Hindrance and Hydrogen Bonding in the Formation of Supramolecular Bottle Brush Polymers. *Macromolecules*, 2013, 46 (19), pp.7911–7919. 10.1021/ma401167n . hal-01696694

HAL Id: hal-01696694

<https://hal.science/hal-01696694>

Submitted on 27 Aug 2020

HAL is a multi-disciplinary open access archive for the deposit and dissemination of scientific research documents, whether they are published or not. The documents may come from teaching and research institutions in France or abroad, or from public or private research centers.

L'archive ouverte pluridisciplinaire **HAL**, est destinée au dépôt et à la diffusion de documents scientifiques de niveau recherche, publiés ou non, émanant des établissements d'enseignement et de recherche français ou étrangers, des laboratoires publics ou privés.

Competition Between Steric Hindrance and Hydrogen Bonding in the Formation of Supramolecular Bottle Brush Polymers

*Sylvain Catrouillet^a, Cécile Fonteneau^a, Laurent Bouteiller^b, Nicolas Delorme^a, Erwan Nicol^a,
Taco Nicolai^b, Sandrine Pensec^b and Olivier Colombani^{a*}*

^a LUNAM Université, Université du Maine, IMMM – UMR CNRS 6283, Université du Maine,
av. O. Messiaen, 72085 Le Mans cedex 9, France.

^b UPMC Univ Paris 6, UMR 7610, Chimie des Polymères, 75005 Paris, France, and CNRS,
UMR 7610, Chimie des Polymères, 75005 Paris, France

KEYWORDS. Self-assembly, urea, supramolecular, bottle-brush, nanotubes.

ABSTRACT.

The formation of supramolecular bottle-brush polymers consisting of a non covalent backbone assembled through directional hydrogen bonds and of poly(isobutylene) (PIB) side-chains was investigated in cyclohexane by light scattering. Two limiting cases were observed depending on the balance between the favorable formation of hydrogen bonds and the unfavorable stretching of the PIB chains within the supramolecular bottle-brushes, in agreement with a theoretical model developed by Wang et al. On one hand, a bisurea self-assembling unit able to form four cooperative

hydrogen bonds per molecule led to relatively short supramolecular bottle-brushes, the length of which could be varied by modifying steric hindrance or by using solvent mixtures. On the other hand, supramolecular bottle-brush polymers exhibiting persistent lengths of more than 300 nm could be obtained by using trisureas that are able to form six hydrogen bonds per molecule. Their easy synthesis and the fact that it is possible to control their self-assembly into long supramolecular bottle-brush polymers make polymer-decorated bisureas and trisureas an attractive alternative to cyclopeptides and shape-persistent rings for the creation of supramolecular nanostructures.

Introduction

Supramolecular polymers are polymer-like architectures resulting from the non covalent directional self-assembly of small molecules.¹⁻⁴ When the non covalent interactions are not too strong, the self-assembly remains reversible and structures are obtained under thermodynamic equilibrium. The strength of the interactions can be tuned in solution by changing temperature, concentration or solvent nature, which facilitates the elaboration of self-healing⁵ or stimuli responsive materials⁶⁻⁹. Moreover, self-assembly may lead to the formation of complex architectures from much simpler molecular building blocks, thus avoiding painstaking synthetic procedures.¹⁰⁻¹²

In particular, covalent bottle-brush polymers are not easy to obtain by conventional synthetic methods.¹³⁻¹⁵ The design of bottle-brush polymers using non covalent interactions has therefore recently been the subject of growing interest. Many reports focused on the design of bottle-brush polymers consisting of a covalent backbone bearing side-chains connected through non covalent interactions.¹⁶⁻¹⁷ More recently, examples of supramolecular bottle-brush polymers where the

backbone itself is formed through directional non covalent interactions have been reported.¹⁸⁻³⁶ In these examples, the non covalent growth of the backbone is mainly promoted by the self-assembly of shape persistent macrocycles through π -stacking^{29-32, 34-35} or by the self-assembly of cyclic oligopeptides through hydrogen bonding^{18,28,33}. Tian et al.³⁶ studied self-assembling units consisting of a π -conjugated part decorated by hydrogen bonding linear oligopeptides.

Wang et al.³⁷ proposed a model for the self-assembly of polymers bearing associating head groups able to self-assemble into linear arrays, which may apply to bottle-brush polymers consisting of a supramolecular backbone. Self-assembly is determined by the competition between the favorable decrease of the free energy of the system due to attractive interactions between the head groups and a non favorable increase of the free energy due to a loss of translational entropy when the unimers gather into a micelle. In addition, for high aggregation numbers the chains need to stretch which reduces their conformational entropy. This effect is stronger for cylindrical than for spherical aggregates and therefore two limiting cases are observed depending on the balance between the loss of conformational entropy due to chain stretching and the free energy gain due to self-assembly. In one limiting case where the interaction between the associating groups is sufficiently strong to overcome the loss of conformational entropy, large rod-like aggregates are predicted to form. The existence of caps at the end of the cylinders reduces some of the loss of conformational entropy because the chains are less stretched in the caps than in the middle of the cylinders. As a consequence, when the steric hindrance increases (longer side-arms, higher grafting density) the model predicts a decrease of the aggregation number of the bottle-brushes. This prediction has actually been observed experimentally for cyclic oligopeptides bearing one to four polymeric side-arms of various lengths.^{20-21,25,27} In these examples, Atomic Force Microscopy (AFM) and Transmission Electron Microscopy (TEM) have been used to characterize the dried structures

after solvent-casting on surfaces. A more recent example confirmed the results observed in the dried state directly in solution using a combination of light and neutron scattering.²³ It is also worth noting that supramolecular bottle-brushes formed by the self-assembly of cyclic oligopeptides decorated with poly(acrylic acid) side-arms became shorter at higher pH because electrostatic repulsion between the charged poly(sodium acrylate) chains increased.²⁴ Finally, the length of amyloid fibrils has been reduced by attaching poly(oxyethylene) side-chains onto them through ionic interactions.³⁸

The second limiting case predicted by Wang et al. is observed when the interaction between the associating groups cannot fully balance the loss of conformational entropy due to chain stretching. In this case, only small star-like aggregates can be formed. Moreover, their aggregation number depends only weakly on the polymer concentration. To our knowledge, this second limiting case has not been observed experimentally.

The present paper focuses on bisurea self-assembling units decorated by poly(isobutylene) (PIB) side chains. Bisureas, consisting of two urea molecules connected by an aromatic ring, are very promising candidates for the design of supramolecular bottle-brushes. First, their synthesis³⁹ is much simpler than that of cyclic oligopeptides⁴⁰⁻⁴¹ or shape persistent macrocycles.⁴² Moreover, a low molar mass bisurea substituted by two non polymeric 2-ethylhexyl side chains (U2PIB0, see Figure 1) has been shown to self-assemble into one-dimensional structures through hydrogen bonds.⁴³⁻⁴⁵ U2PIB0 molecules exchange rapidly within the supramolecular assemblies according to rheology⁴⁶⁻⁴⁷ and isothermal titration calorimetry⁴⁸⁻⁴⁹, thus leading to one-dimensional structures under thermodynamic equilibrium. Moreover, U2PIB0 molecules self-assemble following a cooperative open-association model.⁴⁸⁻⁵⁰ This model predicts in solution the growth of the supramolecular assemblies with increasing concentration and the formation of very long supramolecular polymers

at higher concentrations, which was confirmed experimentally by rheology^{46, 51}, static light scattering⁵²⁻⁵⁴ and Scanning Tunneling Microscopy.⁵⁵ Preliminary results have recently been obtained both in solution⁵⁶ and in the bulk⁵⁷ for U2PIB2 (Figure 1), a bisurea bearing two poly(isobutylene) side chains. It was shown by small angle neutron scattering in toluene at 11 g/L that U2PIB2 self-assembled into small objects exhibiting a weight average aggregation number of 8.5. However, although the model of open association which applies for U2PIB0 predicts that U2PIB2 should eventually form very long supramolecular bottle-brushes at high concentrations, such concentrations were not investigated. Moreover, according to the theory of Wang et al. described above, U2PIB2 may never be able to form long structures if the hydrogen bonds between bisurea units are not strong enough to overcome the stretching penalty of the PIB side-chains.

In order to know whether it is possible to form long supramolecular bottle-brushes using bisurea-based molecules, the self-assembly of U2PIB2 and of two related molecules was investigated directly in solution using light scattering. The two limiting cases predicted by Wang et al. were actually observed depending on the strength of the hydrogen bonds or the steric hindrance of the PIB side chains. It will be shown that U2PIB2 does not form very long supramolecular bottle-brush polymers, because the growth is inhibited beyond a critical length. Structures exhibiting persistent lengths of more than 300 nm were however obtained by replacing bisureas with trisureas (see Figure 1). We believe this new family of supramolecular bottle-brush polymers to be very promising for future applications due to its ease of preparation.

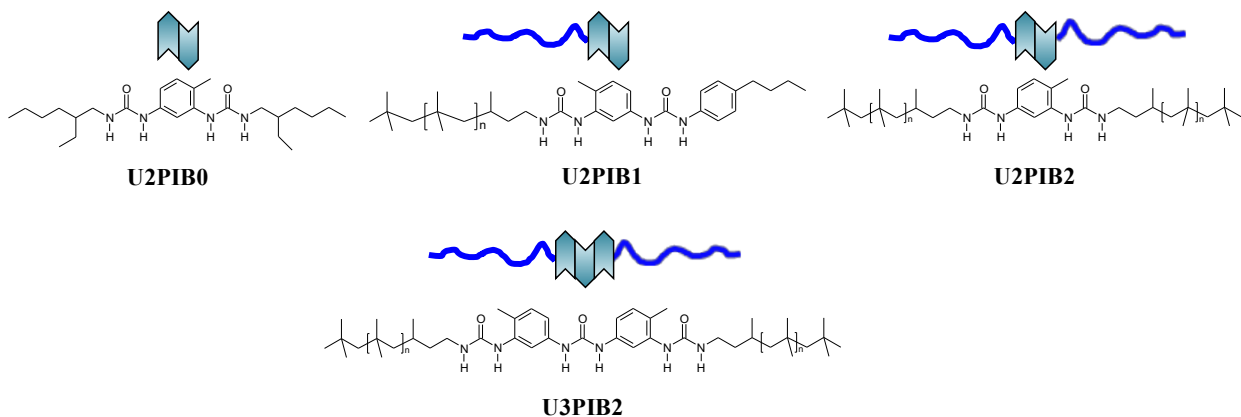


Figure 1. Schematic representation and chemical structures of U_xPIB_y molecules consisting of $x = 2$ or 3 hydrogen bonding units (urea functions) decorated with $y = 0, 1$ or 2 poly(isobutylene) side-chains. Note that U2PIB0 and U2PIB2 have respectively been called EHUT³⁰ and PIBUT⁵⁶⁻⁵⁷ in previous references. The urea functions are represented in antiparallel conformation as recently suggested for bisureas^{47,58} and trisureas⁵⁹ respectively.

Materials and Methods

Materials. Analytical grade solvents were used in all cases. THF and ether were dried over calcium hydride and distilled. 2,4-Toluene diisocyanate (98%, Aldrich), triethylamine (99%, Aldrich) and silica gel (column chromatography grade, Aldrich) were used as received. 4-*n*Butylaniline (Aldrich) was distilled before use. The amino-functional poly(isobutylene) (PIB-NH₂, Kerocom PIBA, ~60%w/w solution in hydrocarbons) was kindly supplied by BASF.

Chemical Characterization.

¹H NMR spectra were recorded on Brüker AC200 (200MHz), Brüker AC400 (400 MHz) or Brüker AC500 (500 MHz) spectrometers at 20°C.

The SEC analyses were performed on a system equipped with a flow refractive index detector (RID10A from Shimadzu) and a miniDAWN TREOS Light Scattering (LS) detector from Wyatt operating at three scattering angles (49° , 90° , 131°) and at a wavelength of 658 nm. The samples were analyzed in THF at room temperature using a flow rate of $1 \text{ mL}\cdot\text{min}^{-1}$ with a Prominence HPLC system from Shimadzu. Polymers were generally injected at a concentration of $\sim 7 \text{ mg}\cdot\text{mL}^{-1}$ in THF after filtration through a $0.2 \mu\text{m}$ pore-size membrane. Separation was performed with a guard column ($5 \mu\text{m}$, $50 \times 7.5 \text{ mm}$) connected to a PLgel Mixed-D column ($5 \mu\text{m}$, $300 \times 7.5 \text{ mm}$) and a PLgel “individual pore size” column ($5 \mu\text{m}$, $50 \times 7.5 \text{ mm}$). The average molar masses (number-average molar mass M_n and weight-average molar mass M_w) and the dispersity ($\mathcal{D} = M_w/M_n$) were derived for all samples from the LS detector using a specific refractive index increment $dn/dc = 0.11 \text{ mL/g}$ for U2PIB2 and U3PIB2 and $dn/dc = 0.12 \text{ mL/g}$ for U2PIB1. The dn/dc values in THF were estimated from the integrated refractive index (RI)-signal knowing the polymer concentration. The values were in very good agreement with those reported in the literature for pure PIB in THF⁶⁰: $dn/dc \sim 0.11 \text{ mL/g}$.

Synthesis.

U2PIB2. The bisurea U2PIB2 was obtained by reacting an excess of PIB-NH₂ (Kerocom PIBA) with 2,4-toluenediisocyanate. The synthesis was performed in solution at room temperature under nitrogen. After purification by precipitation, the structure and purity of the product were confirmed by ¹H NMR spectroscopy and size exclusion chromatography (SEC) in THF. The degree of polymerization, calculated from ¹H NMR signals, was found to be 54 (i.e., $n = 27$, $M_n = 3500 \text{ g}\cdot\text{mol}^{-1}$). SEC in THF was in good agreement with the ¹H NMR results: $M_n = 3300 \text{ g/mol}$, $M_w = 3900 \text{ g/mol}$, $\mathcal{D} = 1.18$. Details of the synthesis and characterization have previously been published.⁵⁶

U2PIB1. A mono-isocyanate/mono-urea, **A** see Figure 2, was first synthesized from a one-step selective reaction between 4-*n*-butyl aniline and one isocyanate function of 2,4-toluene diisocyanate. Details of the synthesis have previously been published (see product **2** in ref.⁶¹). **A** (2.24g, 6.9 mmol) was added at 0°C and under nitrogen to a stirred solution of PIB-NH₂ (Kerocom PIBA) (10 mL corresponding to ~ 4.5 mmol – the molar amount of –NH₂ functions is not very accurate because the concentration of PIB-NH₂ in Kerocom PIBA is not precisely known. PIB-NH₂ was however the limiting reagent.) in dry THF (125 mL) and triethylamine (1.8 mL, 12.9 mmol). The reaction mixture was stirred for two hours at room temperature. 30 mL silica were added and the mixture was stirred for two hours in order to remove **A** molecules in excess by reaction with silica. After removal of the silica by filtration and concentration of the solution, the polymer was precipitated in ethyl acetate (250 mL). The solid product was separated, diluted in a minimum of THF and precipitated again in ethyl acetate. The precipitate was filtered off and dried under vacuum yielding 2.93 g of a white solid.

¹H NMR (200MHz, CDCl₃/d₆-DMSO): δ (ppm) = 8.11 (s, 1H, Ar-NH), 7.98 (s, 1H, Ar-NH), 7.64 (d, 1H, Ar-H), 7.30-7.22 (dd, 1H, Ar-NH, d, 2H, Ar-H), 7.12 (s, 1H, Ar-NH), 7.00-6.96 (d, 2H, Ar-H), 6.91 (d, 1H, Ar-H), 5.61 (s, 1H, CH₂-NH), 3.13 (m, 2H, C H₂-NH), 2.44 (m, 2H, H₂-Ar), 2.01 (s, 3H, Ar-CH₃), 1.6-0.7 (m, 222H, -CH(CH₃)-CH₂-, -C(CH₃)₂-CH₂-, and C(CH₃)₃-CH₂-). The degree of polymerization, calculated from ¹H NMR signals, was found to be 25 (i.e., n = 25, M_n = 1850 g.mol⁻¹). SEC in THF was in good agreement with the ¹H NMR results: M_n = 2000 g/mol, M_w = 2450 g/mol, Đ = 1.2.

U3PIB2. First, a diisocyanate/mono-urea, **B** see Figure 2, was synthesized by partial hydrolysis of 2,4-toluenediisocyanate (TDI) with water as follows.⁶² Water (21.6 mmol, 0.39 mL) in anhydrous ether (150 mL) was added dropwise under argon and at room temperature to a stirred

solution of 2,4-toluenediisocyanate (49.8 mmol, 7.11 mL) in anhydrous ether (45 mL). The solution was stirred overnight and a white precipitate was observed. The precipitate was filtered, rinsed with anhydrous ether and dried under vacuum, yielding 4.4 g of **B**.

U3PIB2 was then obtained by reacting **B** (13.6 mmol, 4.38g) in anhydrous THF (140 mL) with PIB-NH₂ (83 g in hydrocarbons) under argon for 24h. After precipitation in ethyl acetate, a white rubbery solid was obtained (30g).

¹H NMR (200MHz, CDCl₃/d₆-DMSO) δ (ppm) : 8.3 (m, Ar-NH-CO), 7.5 (Ar-H), 7.20 (m, Ar-H), 7.0 (m, Ar-H), 6.8 (Ar-NH-CO), 5.56 (s, CH₂-NH), 2.99 (m, CH₂-NH), 1.97 (s, Ar-CH₃), 0.5-1.5 (m, -CH(CH₃)-CH₂-, -C(CH₃)₂-CH₂)_n and C(CH₃)₃-CH₂-). Integration of the ¹H NMR signals was not trustworthy for U3PIB2 which partially self-assembled even in this solvent mixture. No DP_n could therefore be determined by ¹H NMR. The structure of the polymer was thus confirmed in this case by MALDI TOF-MS.

MALDI-TOF (dithranol, Na): M_{exp(for n=12)} = 1305.397 g/mol, M_{th(for n=12)} = 1305.143 g/mol. Note that only the smallest chains could be detected by MALDI TOF-MS so that M_{exp(for n=12)} does not correspond to the number-average molecular weight of the polymer, but to the molecular weight of one of the most intense signals.

¹³C NMR (50MHz, CDCl₃/d₆-DMSO) δ (ppm) : 156.2 (Ar-NH-CO-NH-CH₂), 122.8 (Ar-CH₃), 153.5 (Ar-NH-CO-NH-Ph), 138.2 (Ar-NH), 138.0 (Ar-NH), 130.6 (Ar-H), 114.2 (Ar-H), 112.8 (Ar-H), 58.7 (-C(CH₃)₂-CH₂)_n, 57.2 (CH₂-CH(CH₃)-CH₂), 37.1 (-C(CH₃)₂-CH₂)_n, 34.8 (N-CH₂-CH₂), 31.7 (-C(CH₃)₃), 31.6 (-C(CH₃)₃), 30.4 (-C(CH₃)₂-CH₂)_n, 25.7 (CH₂-CH(CH₃)-CH₂), 22.0 (CH₂-CH(CH₃)-CH₂), 16.6 (Ar-CH₃).

SEC in THF: M_n = 3000 g/mol, M_w = 3250 g/mol, Đ = 1.07.

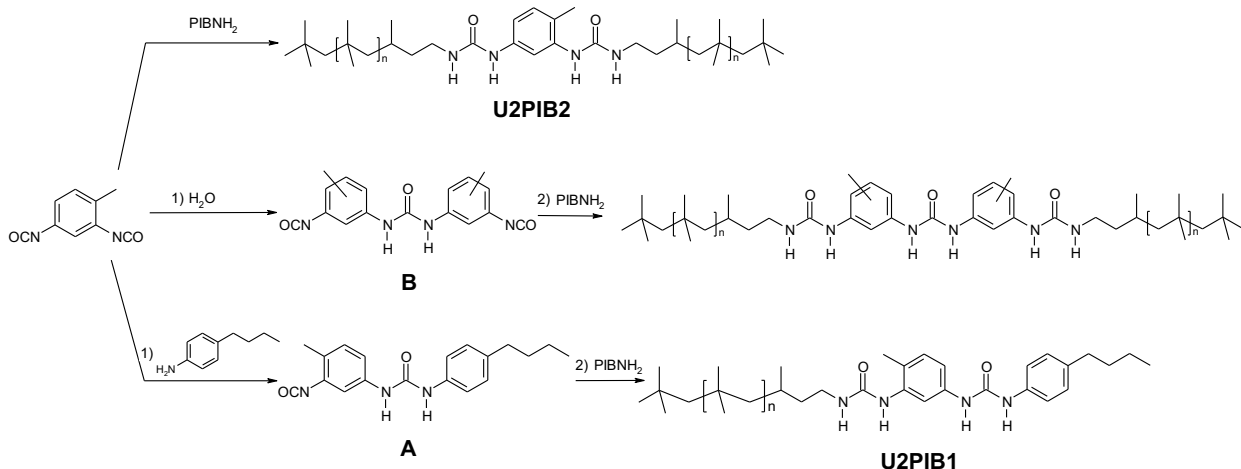


Figure 2. Reaction scheme of the three compounds studied: U2PIB2, U2PIB1 and U3PIB2.

Preparation of the solutions.

Stock polymer solutions in cyclohexane were prepared at 10 or 100 g/L by direct dissolution of the polymer at room temperature. When solvent mixtures were used and whenever possible, the mixture was prepared first and then used both to dissolve and to dilute the polymer in order to avoid risks of compositional drift. The polymer dissolved spontaneously and stable solutions were obtained within 2-24 h depending on the solvent composition, concentration and polymer. The solutions were then filtered through 0.2 μm pore size Acrodisc filters. Dilutions were made by adding filtered solvents (0.2 μm) and stirring for a few minutes. The diluted solutions thus prepared could be measured directly and remained stable for weeks after their preparation. Solutions directly prepared at 10 g/L gave the same results as solutions diluted to 10 g/L from a stock solution at 100 g/L.

Light scattering. Light scattering measurements were done using an ALV-CGS3 system operating with a vertically polarized laser with wavelength $\lambda=632$ nm. The measurements were

done at 20°C over a range of scattering wave vectors ($q=4\pi n \cdot \sin(\theta/2)/\lambda$, with θ the angle of observation and n the refractive index of the solvent) varying from $4.8 \cdot 10^6 \text{ m}^{-1}$ to $2.8 \cdot 10^7 \text{ m}^{-1}$.

Dynamic Light Scattering (DLS). The normalized electric field autocorrelation functions ($g_1(t)$) obtained by dynamic light scattering (DLS) measurements were analysed in terms of a relaxation time (τ) distribution:

$$g_1(t) = \int A(\tau) \exp(-t/\tau) d\tau$$

In all solutions we observed only one q^2 -dependent relaxation mode, which was caused by cooperative diffusion of the solute. This relaxation mode could be well described by a log normal distribution of relaxation times (τ). The apparent diffusion coefficient D was calculated from the average relaxation rate of this relaxation mode as $D=\langle\tau^{-1}\rangle/q^2$. D is related to the apparent hydrodynamic radius, R_a , of the solute:

$$R_a = \frac{kT}{6\pi\eta D} \quad (\text{equation 1})$$

with k Boltzmann's constant, T the absolute temperature and η the viscosity of the solvent. When the particles are small compared to q^{-1} and the solutions are sufficiently dilute so that interactions can be neglected R_a is equal to the z-average hydrodynamic radius, R_z . In that case the relaxation time distribution can be transformed in a distribution of the hydrodynamic radii weighted by the scattering intensity, $A(R_z)$, using equation 1.

Static Light Scattering (SLS). The Rayleigh ratio, R_θ , of the solution was determined following equation (2).

$$R_\theta = \frac{I_{\text{solution}}(\theta) - I_{\text{solvent}}(\theta)}{I_{\text{toluene}}(\theta)} \cdot \left(\frac{n_{\text{solvent}}}{n_{\text{toluene}}} \right)^2 \cdot R_{\text{toluene}} \quad (\text{equation 2})$$

with I_{solution} , I_{solvent} , I_{toluene} the average intensities scattered respectively by the solution, the solvent and the reference (toluene), $n_{\text{solvent}} = 1.426$ (cyclohexane) and $n_{\text{toluene}} = 1.496$ the respective refractive indexes of the solvent and of toluene and $R_{\text{toluene}} = 1.35 \times 10^{-5} \text{ cm}^{-1}$ the Rayleigh ratio of toluene for a wavelength $\lambda = 632.8 \text{ nm}$. For cyclohexane solutions containing small amounts of ethanol, n_{solvent} was taken equal to $n_{\text{cyclohexane}}$.

At a given concentration C , R_{θ} is related to the apparent weight average molecular weight of the scatterers, M_a , and to the structure factor, $S(q)$, which depends on the scattering wave vector according to equations (3) and (4).⁶³ Note that the apparent molecular weight M_a corresponds to the true molecular weight M_w only in very dilute solutions where the interactions between the scatterers can be neglected. At higher concentration, interactions cause M_a to differ strongly from M_w .⁶⁴

$$R_{\theta} = K \cdot C \cdot M_a \cdot S(q) \quad (\text{equation 3})$$

with C the polymer concentration in g/L and K a constant:

$$K = \frac{4\pi^2 n_{\text{solvent}}^2}{\lambda^4 N_a} \left(\frac{\partial n}{\partial C} \right)^2 \quad (\text{equation 4})$$

where N_a is Avogadro's number.

For U2PIB2 and U2PIB1, the scatterers were small, so that their apparent radius of gyration R_g verified $q \cdot R_g < 1$. In this case, equation (3) could be approximated to equation (5) corresponding to the Zimm approximation.⁶⁴ Plotting KC/R_{θ} as a function of q^2 for each concentration yielded the apparent radius of gyration R_g of the scatterers as well as their apparent molecular weight extrapolated to zero angle, M_a . Representative plots are shown for U2PIB2 and U2PIB1 in Supporting Information. The angular dependence was actually negligible within experimental

error for U2PIB2 so that R_g could not be determined accurately. This indicated that $R_g < 20$ nm for U2PIB2. For U2PIB1, accurate determination of R_g was possible since $R_g > 20$ nm and $q.R_g < 1$.

$$\frac{KC}{R_\theta} = \frac{1}{M_a \cdot S(q)} = \frac{1}{M_a} \left(1 + \frac{q^2 \cdot R_g^2}{3} \right) \quad (\text{equation 5})$$

For U3PIB2, the scatterers were very large ($q.R_g > 1$ over the whole q -range investigated) so that the Zimm approximation (equation 5) was no more applicable. In this case, the q -dependency of R_θ/KC gives an information about the shape of the scatterers.⁶⁵ For the lowest concentrations investigated for U3PIB2, R_θ/KC was proportional to q^{-1} over the whole q -range, indicating that this molecule self-assembled into rod-like objects with a persistent length larger than 300 nm.^{65,66} For these low concentrations, the molecular weight per unit of length, M_{lin} , could be determined from the log-log plot of R_θ/KC as a function of q according to equation (6).

$$\frac{R_\theta}{KC} = M_{lin} \cdot \pi \cdot q^{-1} \quad (\text{equation 6})$$

Differential Refractometry. Measurements were performed on an OptiLab rEX from Wyatt Technology Corporation ($\lambda_0=632\text{nm}$). The refractive index increment was measured in cyclohexane at various concentrations of U2PIB2 ranging from 1 to 5 g/L. In cyclohexane, $\partial n/\partial C = 0.10 \text{ mL} \cdot \text{g}^{-1}$, which is in agreement with the value found in the literature for PIB in this solvent.⁶⁰ Consequently, the same values were used for the refractive index increment of U2PIB1 and U3PIB2 whose structure is close to that of U2PIB2.

Isothermal Titration Calorimetry (ITC). Heats of dissociation were measured using a MicroCal VP-ITC titration microcalorimeter. The sample cell (1.435 mL) was filled with pure solvent. A

relatively concentrated U2PIB2 solution in the same solvent was placed in a 295 μL continuously stirred (310 rpm) syringe. Aliquots of the solution were automatically injected into the sample cell, until the syringe was empty.⁴⁸⁻⁴⁹

Results

Self-assembly of U2PIB2 in cyclohexane. First, the self-assembly of U2PIB2 was studied at 20 °C by static and dynamic light scattering in cyclohexane, a non polar solvent where hydrogen bonds are favored. In this solvent, only one diffusive mode of relaxation was observed by dynamic light scattering (DLS) down to 2 g/L. A broad concentration range (2-100 g/L) was studied in order to investigate the influence of the concentration on the self-assembly of U2PIB2. The scattering intensity was too low for accurate measurement below 2 g/L, but isothermal titration microcalorimetry (ITC) in cyclohexane revealed that the self-assembly of U2PIB2 started at 0.04 g/L or even below (See Supporting Information).

Figure 3 shows the concentration dependence of M_n and R_n obtained from light scattering measurements as explained in the Materials and Methods section. M_n and R_n are apparent values which correspond to the molar mass, M_w , and the hydrodynamic radius, R_h , of the solute only when interactions between the scatterers can be neglected, that is in the dilute regime. A variation of M_n and R_n with increasing concentration may be due to a change of M_w and R_h and/or to interactions between the scatterers.

For all concentrations investigated, the scattering intensity did not depend on the scattering wave vector, indicating that the aggregates were small ($R_n < 20$ nm). M_n was almost constant between 2 and 10 g/L and then decreased strongly with further increase of the concentration. The decrease is caused by repulsive, excluded volume, interactions between the scatterers. Therefore the values of

M_n above 10 g/L do not represent the true molar mass of the solute and are not further discussed here.

In the concentration range from 2 to 10 g/L M_n represents the true molar mass of the aggregates which does not depend significantly on the concentration: $M_w = 42\,000$ g/mol. U2PIB2 unimers ($M_w = 3900$ g/mol) thus self-assembled in cyclohexane into small objects of which the aggregation number remained constant ($N_{agg} = M_w(\text{aggregates})/M_w(\text{U2PIB2}) = 11$) at least in the concentration range 2-10 g/L. This aggregation number is in good agreement with the value of 8.5 determined previously by small angle neutron scattering (SANS)⁶⁶ at 11 g/L in toluene, a solvent whose polarity is slightly higher than that of cyclohexane, see Figure 3.

DLS confirmed that the self-assembled structures did not grow significantly between 2 and 10 g/L as the hydrodynamic radius was constant within experimental error and equal to $R_h = 5$ nm (Figure 4). The distribution of hydrodynamic radii derived from the fit, as explained in the materials and methods section, showed that the aggregates were polydisperse, see Figure S4 in the Supporting Information. Note that R_h did not decrease as strongly as M_n with increasing concentration above 10 g/L. This can be explained by the fact that, contrary to the apparent molecular weight, the apparent hydrodynamic radius is influenced both by the excluded volume interactions and by an increase of the friction coefficient with increasing concentration.⁶⁷ The latter leads to an increase of R_h and compensates the decrease caused by excluded volume interactions for the present system.

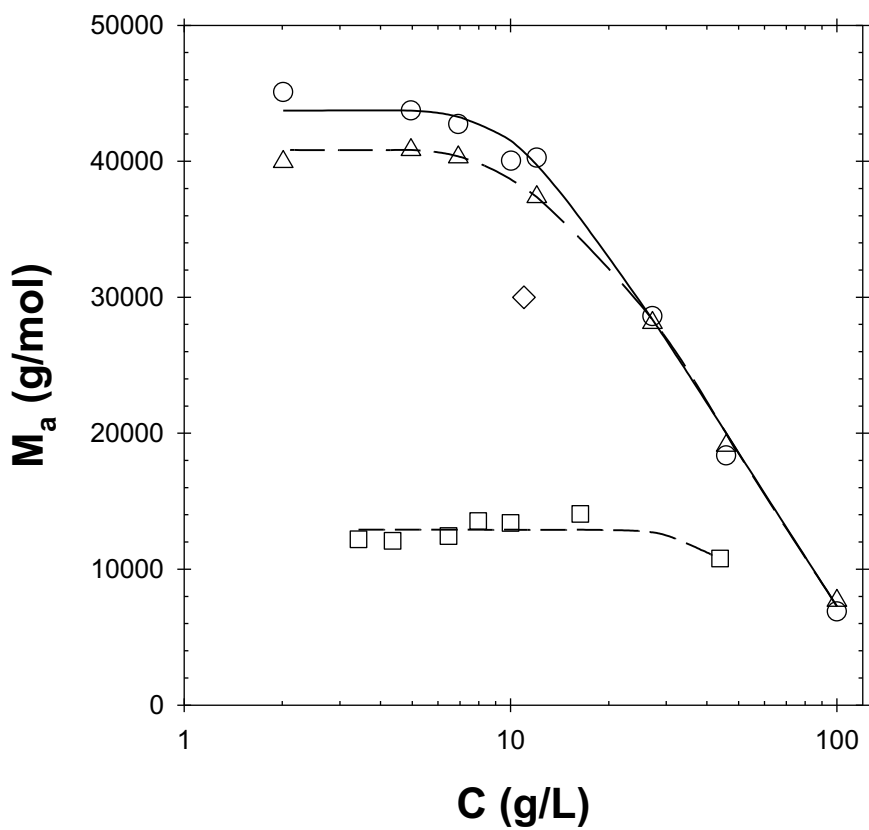


Figure 3. Evolution of the apparent molar mass M_a of U2PIB2 as a function of the polymer concentration obtained by light scattering (○) at 20°C or (△) at 60 °C in cyclohexane and (□) at 20 °C in the presence of 0.25% of ethanol. The diamond (◇) corresponds to previous data obtained by Small Angle Neutron Scattering in toluene- d_8 at room temperature.⁵⁶ The lines are guides to the eyes.

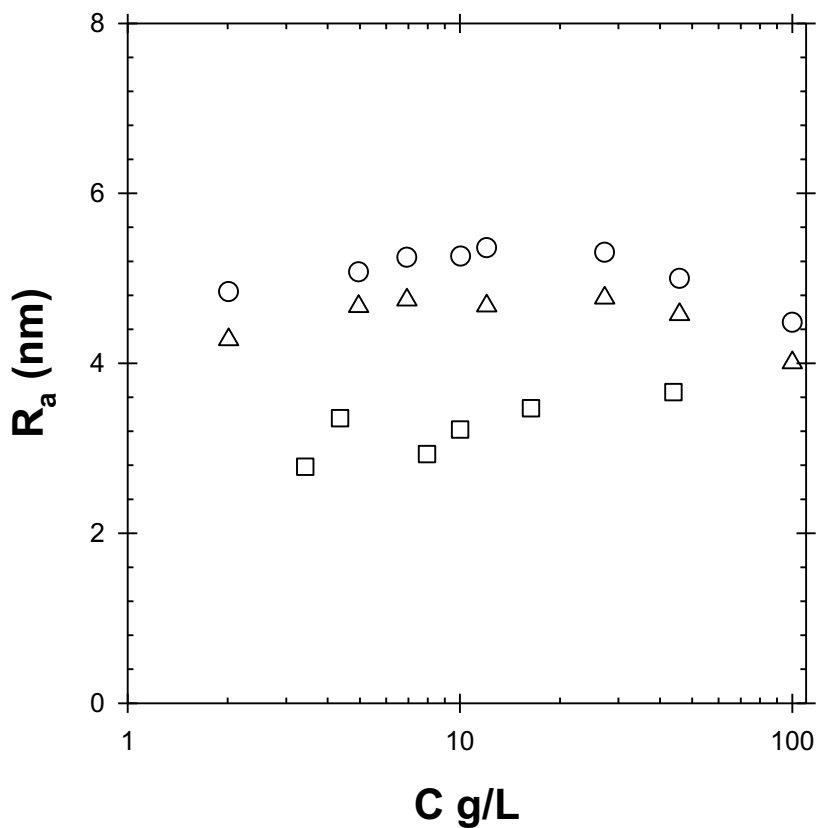


Figure 4. Evolution of the apparent hydrodynamic radius, R_a , with concentration of U2PIB2 (○) at 20°C or (△) at 60°C in cyclohexane and (□) at 20°C in the presence of 0.25% of ethanol.

Isothermal titration microcalorimetry (ITC) of U2PIB2 in cyclohexane (see Supporting Information) revealed that U2PIB2 dissociated at lower concentrations proving that the aggregated structures were formed at thermodynamic equilibrium. This observation excludes the possibility that the molecular weight of U2PIB2 assemblies remained constant between 2 and 10 g/L because they were kinetically frozen. We conclude that U2PIB2 forms structures under thermodynamic equilibrium which self-assemble according to a limited association scenario.

An open-association model was previously proposed to account for the self-assembly of U2PIB2 in solution.⁵⁶ This model fitted nicely with the ITC data obtained for U2PIB2 in chloroform⁵⁶ and toluene (see Supporting Information). It moreover seemed relevant considering the fact that U2PIB2 consists of the same hydrogen bonding part as U2PIB0 (Figure 1) that self-assembles via an open-association model as mentioned in the introduction. However, in view of the present light scattering experiments, it was attempted to fit the ITC results also according to a limited association scenario (see Supporting Information). Provided that a cooperative model⁵⁰ was chosen, for which dimerization is not as favorable as subsequent oligomerization, both a limited and an open association models could fit the ITC data. It can thus be concluded that ITC and LS results are consistent with a limited association scenario. Unfortunately, this also means that ITC cannot be used to distinguish an open from a limited association scenario. ITC should therefore be used with great care when attempting to predict the evolution of the molecular weight of supramolecular assemblies as a function of the concentration unless the open nature of the association can be proven with another technique.

These results indicate that U2PIB2 follows the low-aggregation limiting case described in the model proposed by Wang et al. that was discussed in the introduction. The strength of the hydrogen bonds is, for this system, not sufficient to overcome the stretching penalty required to form very long bottle-brushes. In the following, the steric hindrance and the strength of the hydrogen bonds were altered in order to tune the length of the self-assembled structures.

Effect of the steric hindrance and of the strength of the hydrogen bonds.

Effect of the temperature. Solutions of U2PIB2 in cyclohexane, previously studied at 20°C, were analyzed again at 60°C in order to decrease the strength of the hydrogen bonds. The effect of the

temperature was very weak: only a 10% decrease of the molecular weight and the hydrodynamic radius were observed assuming that the temperature dependence of dn/dc is negligible (Figures 3 and 4). A similar insensitivity to the temperature was also reported by Chapman et al.²³ for cyclic oligopeptides decorated with poly(*n*-butyl acrylate) side-chains.

Effect of the solvent. In order to vary gradually the hydrogen bond competing ability of the solvent, 0-2 wt% ethanol was added to cyclohexane (Figures 5, 6). With 2 wt% ethanol, the supramolecular structures formed by U2PIB2 were fully disrupted as the measured molecular weight was 4000 g/mol, corresponding to that of U2PIB2 unimers determined by SEC ($M_w = 3900$ g/mol). Since ethanol is a non solvent of poly(isobutylene) but a strong hydrogen bond competitor, this confirmed that the self-assembly of U2PIB2 in cyclohexane was driven by hydrogen bonding. More subtle variation of the ethanol content in the cyclohexane/ethanol mixtures resulted in a continuous decrease of the molecular weight (Figure 5) and of the hydrodynamic radius (Figure 6) with increasing ethanol content. Moreover, there was no significant effect of the U2PIB2 concentration on the molecular weight, at least within the range 2-8 g/L, for all ethanol contents. This tendency was confirmed by studying more systematically the effect of the polymer concentration for 0.25/99.75 %wt ethanol/cyclohexane mixtures (Figures 3 and 4), indicating that the true molecular weight is equal to the apparent one and that it hardly varies with the concentration within this concentration range. Again, this behavior is consistent with the low-aggregation limiting case described in the model proposed by Wang et al.

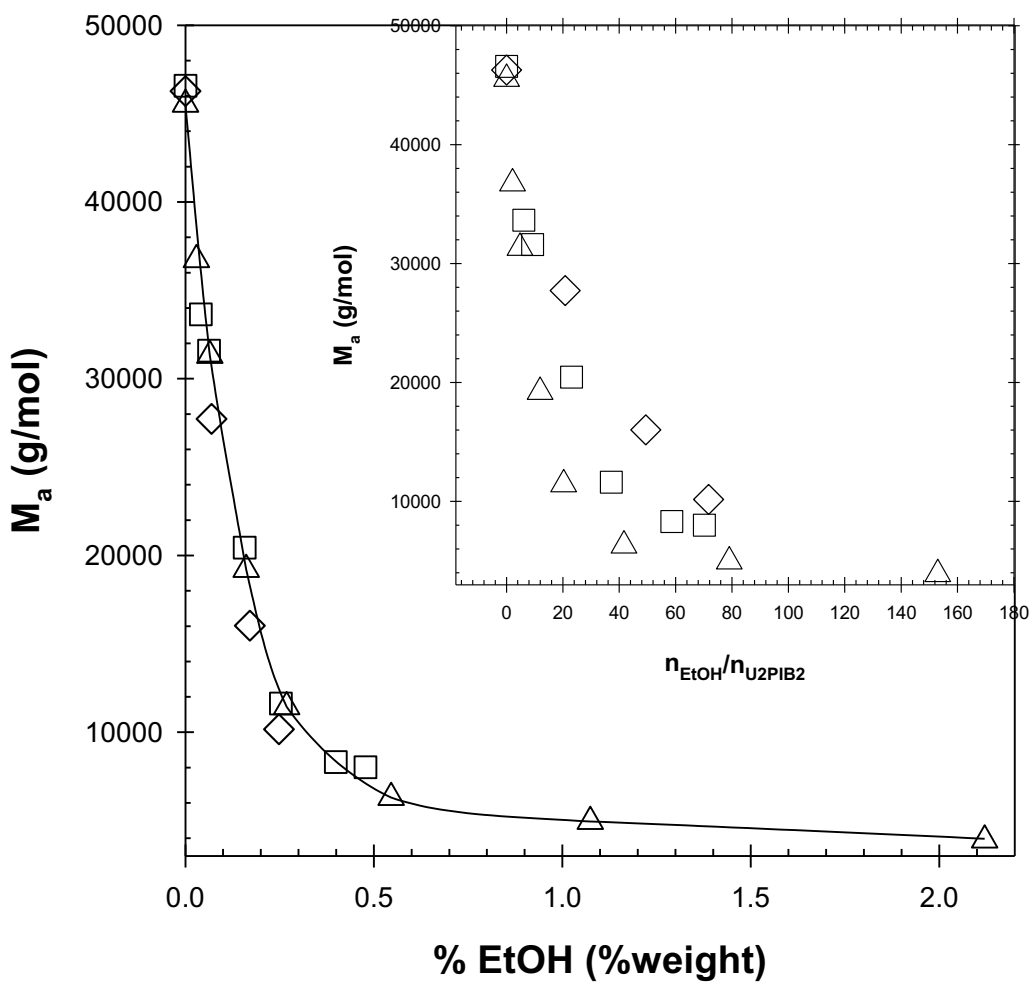


Figure 5. Evolution of the apparent molecular weight, M_a , of U2PIB2 supramolecular assemblies in ethanol/cyclohexane mixtures as a function of the ethanol content and for U2PIB2 concentrations of (\diamond) 2 g/L, (\square) 4 g/L and (\triangle) 8 g/L. (-) Guide to the eyes. Insert: same data represented as a function of the ethanol/U2PIB2 molar ratio.

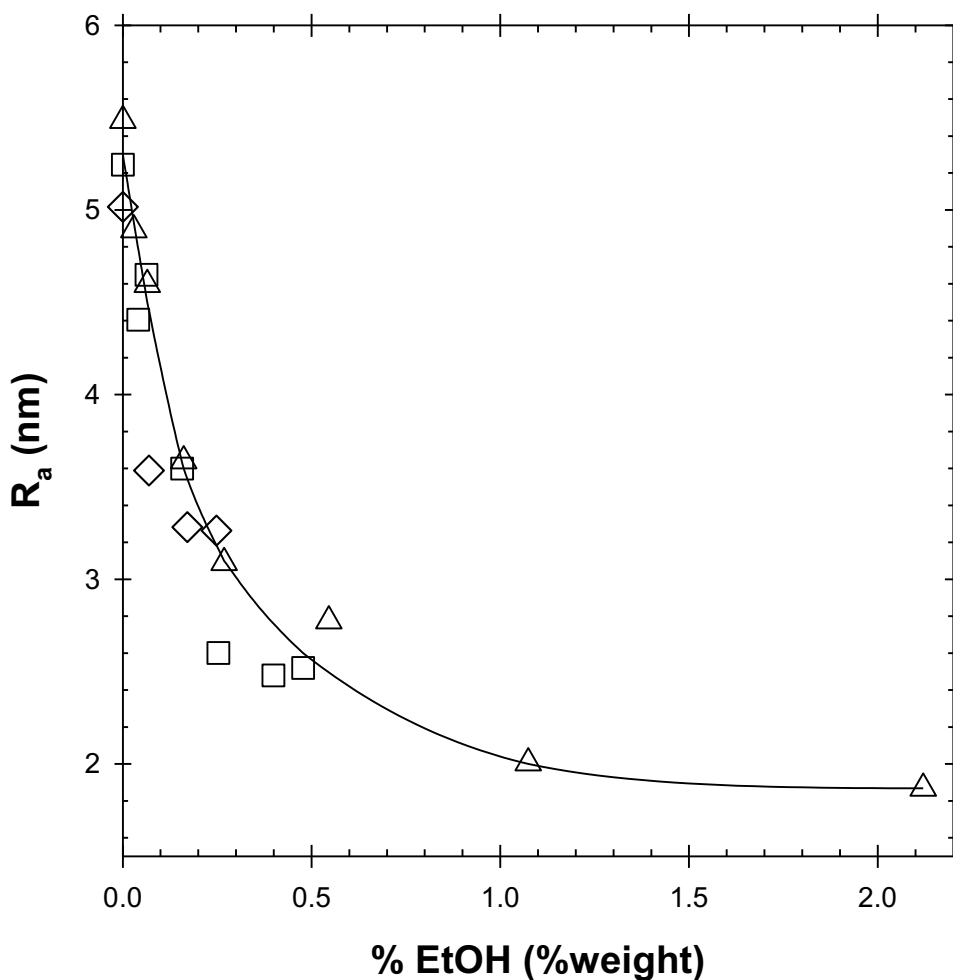


Figure 6. Evolution of the apparent hydrodynamic radius, R_a , of U2PIB2 supramolecular assemblies in ethanol/cyclohexane mixtures as a function of the ethanol content and for U2PIB2 concentrations of (◇) 2 g/L, (□) 4 g/L and (△) 8 g/L. (-) Guide to the eyes.

Notice that ethanol does not act as a strong chain stopper. Indeed, if ethanol were a strong chain stopper, a low ethanol/U2PIB2 molar ratio would significantly reduce the size of the assemblies and this ratio would be expected to rule the apparent molecular weight, independently of the polymer concentration, which is not the case (Insert figure 5).^{51, 53-54, 68} Addition of ethanol simply

enhances the hydrogen bond competing ability of the solvent mixture, which results in a gradual decrease of the molecular weight of the supramolecular assemblies.⁶⁹⁻⁷⁰

Effect of the grafting density (number of arms per bisurea unit). A bisurea bearing only one PIB arm, U2PIB1, (Figure 1) was synthesized and its self-assembly in cyclohexane was studied by light scattering. U2PIB1 also self-assembled in cyclohexane (Figure 7). The apparent molecular weight could not be measured with sufficient accuracy below 0.5 g/L. M_n was almost constant between 0.5 and 5 g/L, but as for U2PIB2, excluded volume interactions caused the apparent molecular weight to decrease at higher concentrations. Here, M_n started to deviate strongly from M_w at a lower concentration than in the case of U2PIB2 because U2PIB1 forms larger assemblies which interact significantly at lower concentrations. In the case of U2PIB1 solutions, the scattered light intensity depended significantly on the scattering wave vector in the accessible range, from which a radius of gyration $R_g = 30$ nm could be deduced that was independent of the polymer concentration for $C < 5$ g/L (see Supporting Information). A very slight increase of M_n and R_g with the concentration indicating limited growth of the assemblies between 0.5 and 5 g/L cannot be excluded. However, this increase is much weaker than the growth predicted for an open association scenario: $M_w \propto C^\alpha$ with $\alpha \geq 0.5$.^{54,71} In first approximation, it may be concluded that $M_n = 230\,000$ g/mol remains constant between 0.5 and 5 g/L for U2PIB1 assemblies, corresponding to an aggregation number $N_{agg} = 100$. As might be expected, the hydrodynamic radius was also larger for U2PIB1 than for U2PIB2: $R_h \sim 11.5$ nm. Also for this system the distribution of hydrodynamic radii derived from the fit showed that the aggregates were polydisperse, see Figure S4 in the Supporting Information.

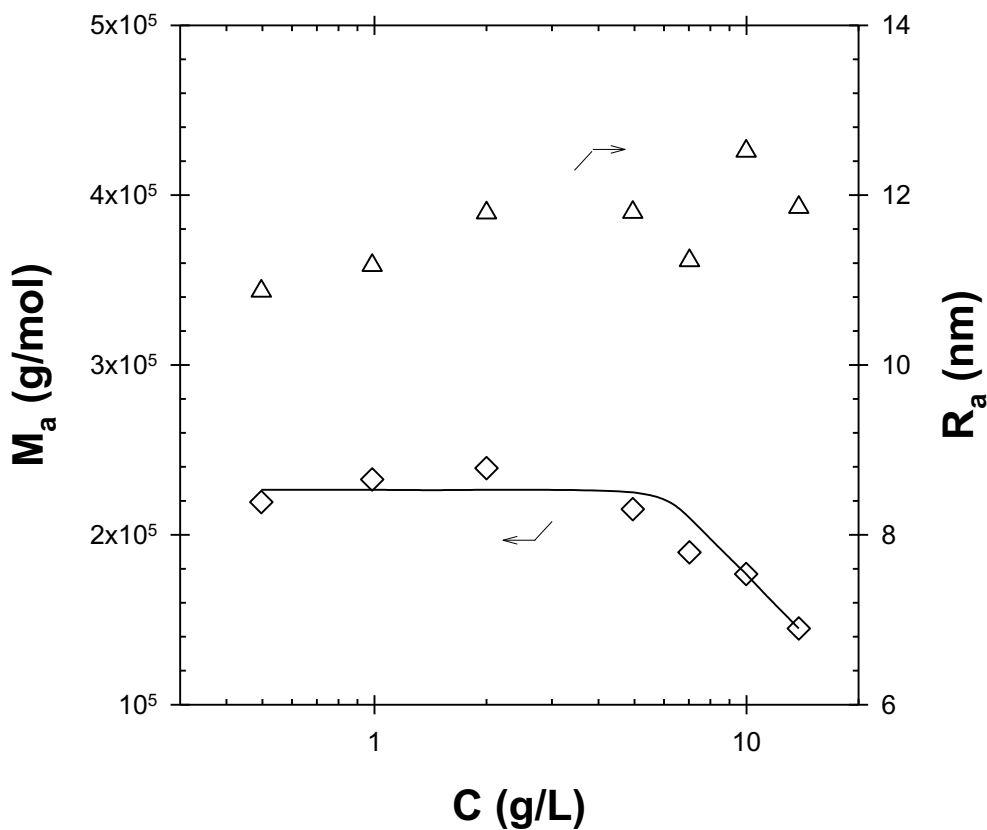


Figure 7. Evolution of the apparent molar mass M_a (\diamond) and of the apparent hydrodynamic radius R_a (\triangle) of U2PIB1 in cyclohexane as a function of the polymer concentration obtained by light scattering at 20°C. The solid line is a guide to the eye.

Effect of stronger hydrogen bonding units. It was previously reported that bisureas self-assemble orders of magnitude more strongly than monoureas.^{39,43} It is therefore expected that the association of trisureas is much stronger than that of bisureas⁵⁹. In order to investigate the effect of the association strength, U3PIB2 (Figure 1), consisting of three urea functions in the associating unit and bearing two PIB chains, was synthesized and characterized. It is to be noted that U3PIB0, consisting of the same associating unit connected to two non polymeric 2-ethylhexyl side-chains

was also synthesized but could not be studied because of its insolubility in common non polar solvents.

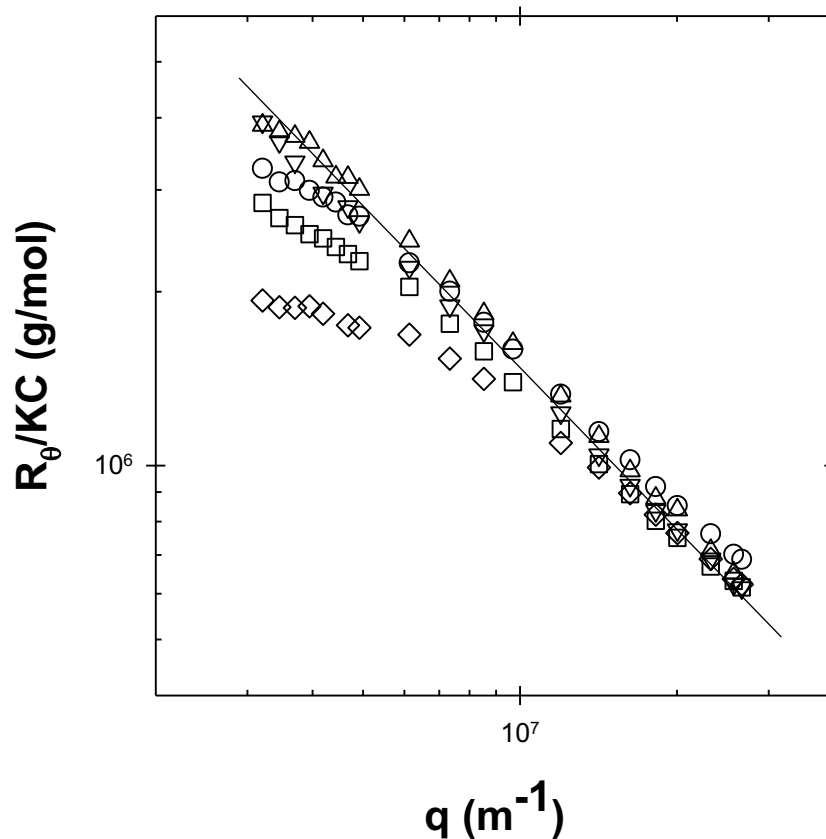


Figure 8. Evolution of R_{θ}/KC of U3PIB2 in cyclohexane as a function of the scattering wave vector q and for different polymer concentrations: (Δ) 0.08 g/L, (∇) 0.14 g/L, (\circ) 0.68 g/L, (\square) 1.34 g/L and (\diamond) 3.41 g/L. The solid line has slope -1.

A q^{-1} dependence of R_{θ}/KC was observed over the whole q -range (0.003 nm^{-1} to 0.03 nm^{-1}) for U3PIB2 solutions at 0.08 and 0.14 g/L. This indicated that U3PIB2 self-assembled into very large structures ($q \cdot R_g > 1$, see Materials and Methods) exhibiting a cylindrical morphology with a persistence length larger than 300 nm (Figure 8). At higher U3PIB2 concentrations, a plateau

appeared at the lowest q values due to the overlapping of the cylinders. This plateau appeared at higher q and corresponded to lower M_n with increasing concentration, indicating that the system became more homogeneous. From the data obtained at the lowest concentrations, the molecular weight per unit of length, M_{in} , could be deduced (see Materials and Methods). Assuming a distance between hydrogen bonded urea-units of 0.46 nm,⁷² the molecular weight between two hydrogen bonding units was calculated to be 2300 g/mol. This value is somewhat lower than the molecular weight of one U3PIB2 unimer ($M_w = 3250$ g/mol). Nevertheless, we may conclude that U3PIB2 formed monodimensional structures consisting of one molecule in the cross-section as do U2PIB2 in toluene⁵⁶ or U2PIB0 in chloroform,⁴⁴ and that these structures were extremely long compared to those formed by U2PIB2.

Discussion

On one hand, U2PIB1 and U2PIB2 form rather small supramolecular structures (in terms of M_w , R_n and R_g) which hardly grow with increasing polymer concentration. These polymers self-assemble according to the low-aggregation number limit described by Wang et al., as mentioned in the introduction. In this case, the strength of the hydrogen bonding is not sufficient to compensate for the conformational entropic penalty of stretching of the side chains. It is nevertheless possible to tune the aggregation of these systems to some extent. Decreasing the strength of the hydrogen bonds by adding a small amount of ethanol to U2PIB2 solutions in cyclohexane indeed leads to even lower aggregation numbers than in pure cyclohexane. On the contrary, decreasing the degree of grafting by removing one PIB arm per repeating unit from U2PIB2 to U2PIB1 leads to longer bottle-brush polymers.

On the other hand, the q^{-1} dependence of R_g/KC for U3PIB2 indicates that these molecules self-assemble into very long supramolecular bottle-brushes according to the high aggregation number limiting case predicted by Wang et al.'s model. The strength of the hydrogen bonds formed in cyclohexane between U3PIB2 molecules could not be evaluated by ITC or Fourier Transformed Infra-Red spectroscopy because the amount of non associated NH groups was negligible. However, it is clear from the light scattering results that their strength must be sufficient to overcome the conformational entropic penalty of stretching of the PIB side-arms so that very long and rigid supramolecular bottle-brushes are formed.

The two limiting cases predicted by Wang et al. could therefore be observed by modifying the chemical structure of the hydrogen bonding unit in these systems. Note also that Wang et al.'s model explains why U2PIB0 with short 2-ethyl hexyl side chains forms very long rod-like aggregates^{46,51-55} contrary to U2PIB2: there is virtually no conformational entropic penalty for the association of U2PIB0 into long cylinders. Accordingly, U2PIB0 self-assembles following an open association scenario, whereas U2PIB2 forms structures whose aggregation number hardly depends on the concentration and is limited to a small value, as predicted by Wang et al. for each limiting case.

The self-assembled structures can be modeled in first approximation as consisting of a cylinder of height h and diameter d end-capped at both ends with spherical caps of diameter d (Figure 9).³⁷ The pertinence of this model is supported by previous small angle neutron scattering (SANS) experiments in toluene,⁵⁶ which showed that U2PIB2 forms very small supramolecular bottle-brush polymers consisting of an array of self-assembled bisurea units with dangling PIB side chains. The length h of the array formed by the self-assembled bisureas can be calculated from the aggregation

number N_{agg} determined by SLS and the distance between two hydrogen bonded bisureas, $e = 0.46$ nm, determined from crystallographic measurements⁷²: $h = (N_{agg} - 1) \times e$. We found $h = 4.5$ nm for U2PIB2 and $h = 45$ nm for U2PIB1, which are weight-average values as N_{agg} . In principle, the value of the hydrodynamic radius R_h determined by dynamic light scattering allows deducing d since the relationship between R_h , d and h is known for the kind of morphologies represented on Figure 9.⁶⁷ However, the aggregates formed by U2PIB2 and U2PIB1 are polydisperse as mentioned above. As a consequence, h , which is a weight-average, and R_h , which is a z-average, cannot be compared quantitatively. Calculating reliable values of d was thus not possible in our case since it would have required precise knowledge of the size distribution of the aggregates which was not available.

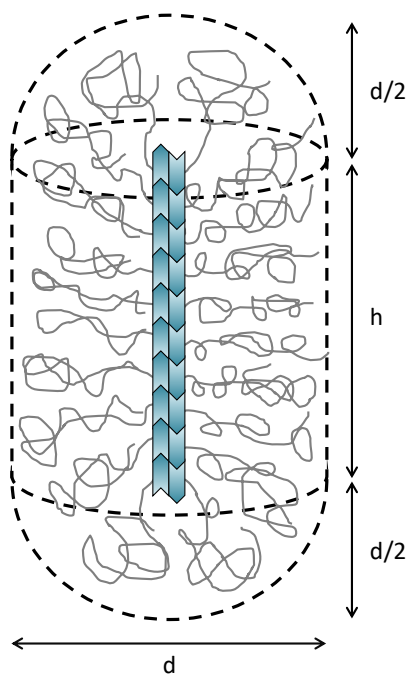


Figure 9. Proposed structure of the supramolecular bottle-brush polymers formed by U2PIB2 and U2PIB1. Note that U2PIB1 actually bears only one PIB arm per bisurea unit.

Conclusion

This paper focused on the self-assembly of bisurea and trisurea molecules, consisting respectively of two or three urea units separated by rigid aromatic rings and functionalized by PIB side-chains, into supramolecular bottle-brushes with a non covalent backbone. The results are in very good qualitative agreement with the two limiting cases predicted by a theory developed by Wang et al.³⁷ indicating that self-assembly depended on the competition between steric hindrance and the strength of the hydrogen bonds.

For U2PIB2 and U2PIB1, the hydrogen bonds between bisureas are not sufficiently strong to compensate the conformational entropic penalty of the PIB side-arms and only rather short structures are formed. Decreasing the number of PIB arms per bisurea from U2PIB2 to U2PIB1 nevertheless increased the aggregation number of the resulting structures by one order of magnitude.

Trisureas seem on the contrary to be very promising building blocks for the preparation of bottle-brush polymers with a supramolecular backbone. Their synthesis is straightforward and they self-assemble sufficiently strongly to allow the formation of very long supramolecular bottle-brushes with a persistence length larger than 300 nm.

ASSOCIATED CONTENT

Supporting Information. a) Isothermal Titration Calorimetry of U2PIB2 in cyclohexane, toluene and chloroform and fits of the data according to a limited or an open association scenario. b) Representative distributions of R_n for U2PIB2 and U2PIB1. c) Determination of R_s and R_g – representative plots for U2PIB2 and U2PIB1 in cyclohexane. This material is available free of charge via the Internet at <http://pubs.acs.org>.

AUTHOR INFORMATION

Corresponding Authors

email: olivier.colombani@univ-lemans.fr

Tel: +33 2 43 83 33 15 / Fax: +33 2 43 83 35 58

Author Contributions

The manuscript was written through contributions of all authors. All authors have given approval to the final version of the manuscript.

Funding Sources

This work has been funded by the Agence Nationale de la Recherche in the frameworks ANR-2011-JS08-006-01 and ANR-10-BLAN-0801.

Notes

Any additional relevant notes should be placed here.

ACKNOWLEDGMENT

The authors thank Magali Martin and Christophe Chassenieux for their help with the SEC analyses and A. Lange and BASF company for the gift of a Kerocom PIBA sample.

REFERENCES

1. Bouteiller, L. *Adv. Polym. Sci.* **2007**, 207, 79.
2. Brunsveld, L.; Folmer, B. J. B.; Meijer, E. W.; Sijbesma, R. P. *Chem. Rev.* **2001**, 101, 4071-4097.
3. Ciferri, A., *Supramolecular Polymers*. Marcel Decker: New York, 2005.

4. De Greef, T. F. A.; Smulders, M. M. J.; Wolffs, M.; Schenning, A. P. H. J.; Sijbesma, R. P.; Meijer, E. W. *Chem. Rev.* **2009**, 109, 5687-5754.
5. Cordier, P.; Tournilhac, F.; Soulie-Ziakovic, C.; Leibler, L. *Nature* **2008**, 451, 977.
6. Burnworth, M.; Tang, L.; Kumpfer, J. R.; Duncan, A. J.; Beyer, F. L.; Fiore, G. L.; Rowan, S. J.; Weder, C. *Nature* **2011**, 472, 334-338.
7. Cantekin, S.; Eikelder, H. M. M. t.; Markvoort, A. J.; Veld, M. A. J.; Korevaar, P. A.; Green, M. M.; Palmans, A. R. A.; Meijer, E. W. *Angew. Chem. Int. Ed.* **2012**, 51, (26), 6426-6431.
8. Aida, T.; Meijer, E. W.; Stupp, S. I. *Science* **2012**, 335, 813-817.
9. Helmich, F.; Lee, C. C.; Nieuwenhuizen, M. M. L.; Gielen, J. C.; Christianen, P. C. M.; Larsen, A.; Fytas, G.; Leclere, P. E. L. G.; Schenning, A. P. H. J.; Meijer, E. W. *Angew. Chem. Int. Ed.* **2010**, 49, 3939-3942.
10. Park, T.; Zimmerman, S. C. *J. Am. Chem. Soc.* **2006**, 128, 13986-13987.
11. Corbin, P. S.; Lawless, L. J.; Li, Z.; Ma, Y.; Witmer, M. J.; Zimmerman, S. C. *Proc. Natl. Acad. Sci.* **2002**, 99, 5099-5104.
12. Percec, V.; Dulcey, A. E.; Balagurusamy, V. S. K.; Miura, Y.; Smidrkal, J.; Peterca, M.; Nummelin, S.; Edlund, U.; Hudson, S. D.; Heiney, P. A.; Duan, H.; Magonov, S. N.; Vinogradov, S. A. *Nature* **2004**, 430, 764-768.
13. Zhang, M.; Müller, A. H. E. *J. Polym. Sci., Part A: Polym. Chem.* **2005**, 43, 3461-3481.
14. Sheiko, S. S.; Sumerlin, B. S.; Matyjaszewski, K. *Prog. Polym. Sci.* **2008**, 33, 759-785.

15. Feng, C.; Li, Y.; Yang, D.; Hu, J.; Zhang, X.; Huang, X. *Chem. Soc. Rev.* **2011**, 40, 1282–1295.
16. Brinke, G. T.; Ikkala, O. *The Chemical Record* **2004**, 4, 219-230.
17. Weck, M. *Polym. Int.* **2007**, 56, 453–460.
18. Cate, M. G. J. t.; Severin, N.; Börner, H. G. *Macromolecules* **2006**, 39, 7831-7838.
19. Chapman, R.; Danial, M.; Koh, M. L.; Jolliffe, K. A.; Perrier, S. *Chem. Soc. Rev.* **2012**, 41, 6023–6041.
20. Chapman, R.; Jolliffe, K. A.; Perrier, S. *Aust. J. Chem.* **2010**, 63, 1169–1172.
21. Chapman, R.; Jolliffe, K. A.; Perrier, S. *Polym. Chem.* **2011**, 2, 1956-1963.
22. Chapman, R.; Jolliffe, K. A.; Perrier, S. *Adv. Mater.* **2013**, 25, 1170–1172.
23. Chapman, R.; Koh, M. L.; Warr, G. G.; Jolliffe, K. A.; Perrier, S. *Chem. Sci.* **Accepted 2013**, DOI: 10.1039/c0xx00000x.
24. Chapman, R.; Warr, G. G.; Perrier, S.; Jolliffe, K. A. *Chem. Eur. J.* **2013**, 19, 1955 – 1961.
25. Couet, J.; Biesalski, M. *Macromolecules* **2006**, 39, 7258-7268.
26. Couet, J.; Biesalski, M. *Soft Matter* **2006**, 2, 1005–1014.
27. Couet, J.; Biesalski, M. *Small* **2008**, 4, (7), 1008–1016.
28. Couet, J.; Jeyaprakash, J. D.; Samuel, S.; Kopyshchev, A.; Santer, S.; Biesalski, M. *Angew. Chem. Int. Ed.* **2005**, 44, 3297 –3301.

29. Dingenouts, N.; Klyatskaya, S.; Rosenfeldt, S.; Ballauff, M.; Höger, S. *Macromolecules* **2009**, *42*, 5900–5902.
30. Fritzsche, M.; Jester, S.-S.; Höger, S.; Klaus, C.; Dingenouts, N.; Linder, P.; Drechsler, M.; Rosenfeldt, S. *Macromolecules* **2010**, *43*, 8379–8388.
31. Höger, S. *Chem. Eur. J.* **2004**, *10*, 1320-1329.
32. Höger, S.; Bonrad, K.; Rosselli, S.; Ramminger, A.-D.; Wagner, T.; Silier, B.; Wiegand, S.; Häussler, W.; Lieser, G.; Scheumann, V. *Macromol. Symp.* **2002**, *177*, 185-191.
33. Loschonsky, S.; Couet, J.; Biesalski, M. *Macromol. Rapid Commun.* **2008**, *29*, 309–315.
34. Rosselli, S.; Ramminger, A.-D.; Wagner, T.; Lieser, G.; Höger, a. S. *Chem. Eur. J.* **2003**, *9*, 3481-3491.
35. Rosselli, S.; Ramminger, A.-D.; Wagner, T.; Silier, B.; Wiegand, S.; Häussler, W.; Lieser, G.; Scheumann, V.; Höger, S. *Angew. Chem. Int. Ed.* **2001**, *40*, (17), 3137-3141.
36. Tian, L.; Szilluweit, R.; Marty, R.; Bertschi, L.; Zerson, M.; Spitzner, E.-C.; Magerled, R.; Frauenrath, H. *Chem. Sci.* **2012**, *3*, 1512–1521.
37. Wang, Z.-G.; Safran, S. A. *J. Chem. Phys.* **1988**, *89*, (8), 5323-5328.
38. Rühs, P. A.; Adamcik, J.; Bolisetty, S.; Sanchez-Ferrer, A.; Mezzenga, R. *Soft Matter* **2011**, *7*, 3571-3579.
39. Lortie, F.; Boileau, S.; Bouteiller, L.; Chassenieux, C.; Demé, B.; Ducouret, G.; Jalabert, M.; Lauprêtre, F.; Terech, P. *Langmuir* **2002**, *18*, 7218-7222.

40. Rovero, P.; Quartara, L.; Fabbri, G. *Tetrahedron Letters* **1991**, 32, 2639-2642.
41. Ghadiri, M. R.; Granja, J. R.; Milligan, R. A.; McRee, D. E.; Khazanovich, N. *Nature* **1993**, 366, 324-327.
42. Höger, S. *Journal of Polymer Science Part A: Polymer Chemistry* **1999**, 37, 2685–2698.
43. Boileau, S.; Bouteiller, L.; Lauprêtre, F.; Lortie, F. *New J. Chem.* **2000**, 24, 845.
44. Bouteiller, L.; Colombani, O.; Lortie, F.; Terech, P. *J. Am. Chem. Soc.* **2005**, 127, 8893-8898.
45. Pinault, T.; Isare, B.; Bouteiller, L. *Chem. Phys. Chem.* **2006**, 7, 816-819.
46. Ducouret, G.; Chassenieux, C.; Martins, S.; Lequeux, F.; Bouteiller, L. *J. Colloid Interface Sci.* **2007**, 310, 624–629.
47. Shikata, T.; Nishida, T.; Isare, B.; Linares, M.; Lazzaroni, R.; Bouteiller, L. *J. Phys. Chem. B* **2008**, 112, 8459–8465.
48. Arnaud, A.; Bouteiller, L. *Langmuir* **2004**, 20, 6858-6863.
49. Bellot, M.; Bouteiller, L. *Langmuir* **2008**, 24, 14176-14182.
50. Simic, V.; Bouteiller, L.; Jalabert, M. *J. Am. Chem. Soc.* **2003**, 125, 13148-13154.
51. Pinault, T.; Cannizzo, C.; Andrioletti, B.; Ducouret, G.; Lequeux, F.; Bouteiller, L. *Langmuir* **2009**, 25, (15), 8404–8407.
52. van der Gucht, J.; Besseling, N. A. M.; Knoben, W.; Bouteiller, L.; Stuart, M. A. C. *Phys. Rev. E.* **2003**, 67, 051106.

53. Knoben, W.; Besseling, N. A. M.; Stuart, M. A. C. *Macromolecules* **2006**, *39*, 2643-2653.
54. Lortie, F.; Boileau, S.; Bouteiller, L.; Chassenieux, C.; Lauprêtre, F. *Macromolecules* **2005**, *38*, 5283-5287.
55. Vonau, F.; Aubel, D.; Bouteiller, L.; Reiter, G.; Simon, L. *Phys. Rev. Lett.* **2007**, *99*, (8), 086103.
56. Pensec, S.; Nouvel, N.; Guilleman, A.; Creton, C.; Boué, F.; Bouteiller, L. *Macromolecules* **2010**, *43*, 2529–2534.
57. Courtois, J.; Baroudi, I.; Nouvel, N.; Degrandi, E.; Pensec, S.; Ducouret, G.; Chanéac, C.; Bouteiller, L.; Creton, C. *Adv. Funct. Mater.* **2010**, *20*, 1803–1811.
58. Brocorens, P.; Linares, M.; Guyard-Duhayon, C.; Guillot, R.; Andrioletti, B.; Suhr, D.; Isare, B.; Lazzaroni, R.; Bouteiller, L. *J. Phys. Chem. B* **2013**, *117*, 5379-5386.
59. Roy, N.; Buhler, E.; Lehn, J.-M. *Chem. Eur. J.* **2013**, *19*, 8814 – 8820.
60. Huglin, *Light Scattering from Polymer Solutions*. Academic press: London, New York, 1972.
61. Colombani, O.; Bouteiller, L. *New J. Chem.* **2004**, *28*, 1373-1382.
62. Pelley, R. L. US 2,757,184, 1956.
63. Brown, W., *Light Scattering. Principles and Development*. Clarendon Press: Oxford ed.; 1996.
64. Brown, W., *Light Scattering. Principles and Development*. Clarendon Press: Oxford, 1996.

65. Higgins, J. S.; Benoit, H. C., *Polymers and Neutron Scattering*. Clarendon Press: Oxford, 1994.
66. Berret, J.-F., Rheology of Wormlike Micelles: Equilibrium Properties and Shear Banding Transitions. In *Molecular Gels*, Weiss, R. G.; Terech, P., Eds. Springer: Netherlands, 2006; pp 667-720.
67. Brown, W., *Dynamic Light Scattering: The Method and Some Applications*. Clarendon Press: Oxford, 1993.
68. Knoben, W.; Besseling, N. A. M.; Bouteiller, L.; Stuart, M. A. C. *Phys. Chem. Chem. Phys.* **2005**, 7, 2390-2398.
69. Buurma, N. J.; Cook, J. L.; Hunter, C. A.; Low, C. M. R.; Vinter, J. G. *Chem. Sci.* **2010**, 1, 242–246.
70. Francisco, K. R.; Dreiss, C. c. A.; Bouteiller, L.; Sabadini, E. *Langmuir* **2012**, 28, 14531–14539.
71. Zhao, D.; Moore, J. S. *Org. Biomol. Chem.* **2003**, 1, 3471-3491.
72. Perez-Folch, J.; Subirana, J. A.; Aymami, J. J. *J. Chem. Crystallogr.* **1997**, 27, 367-369.

FOR TABLE OF CONTENT USE ONLY.

Competition Between Steric Hindrance and Hydrogen Bonding in the Formation of Supramolecular Bottle Brush Polymers.

Sylvain Catrouillet, Cécile Fonteneau, Laurent Bouteiller, Nicolas Delorme, Erwan Nicol, Taco Nicolai, Sandrine Pensec and Olivier Colombani

